

In-plane thermal conductivity of disordered layered WSe_2 and $(\text{W})_x(\text{WSe}_2)_y$ superlattice films

Anastassios Mavrokefalos

Department of Mechanical Engineering, The University of Texas at Austin, Austin, Texas 78712, USA

Ngoc T. Nguyen

Department of Chemistry, Materials Science Institute, University of Oregon, Eugene, Oregon 97403, USA

Michael T. Pettes

Department of Mechanical Engineering, The University of Texas at Austin, Austin, Texas 78712, USA

David C. Johnson

Department of Chemistry, Materials Science Institute, University of Oregon, Eugene, Oregon 97403, USA

Li Shi^{a)}

Department of Mechanical Engineering and Center for Nano and Molecular Science and Technology, Texas Materials Institute, The University of Texas at Austin, Austin, Texas 78712, USA

(Received 30 July 2007; accepted 1 October 2007; published online 26 October 2007)

It was recently reported that misoriented layered WSe_2 and $(\text{W})_x(\text{WSe}_2)_y$ films possess extremely low cross-plane thermal conductivity. Here, we report that the in-plane thermal conductivity results for WSe_2 and $\text{W}_4(\text{WSe}_2)_{10}$ films measured by using a suspended device are about 30 times higher than the cross-plane values because of the in-plane ordered and cross-plane disordered structures and about six times lower than that of compacted single-crystal WSe_2 platelets. The additional W layers in the $\text{W}_4(\text{WSe}_2)_{10}$ films were found to greatly increase the in-plane electrical conductivity relative to the WSe_2 films, but reduce the in-plane lattice thermal conductivity assuming the Wiedemann-Franz law. © 2007 American Institute of Physics. [DOI: 10.1063/1.2800888]

Thin film heterostructures have been widely used in optoelectronic devices and are currently under active investigation for thermoelectric energy conversion applications.^{1,2} It was recently found that the cross-plane thermal conductivity (κ) of disordered WSe_2 thin films is as low as 0.05 W/m K.³ This result is the lowest κ ever reported for a dense solid to this date. The disordered WSe_2 thin films is an expansion of a previous work developed by Johnson and co-workers where a multilayer superlattice structure is formed by interfacial nucleation along the interfaces.^{4,5} The extremely low cross-plane κ is attributed to phonon localization induced by the random stacking of the two-dimensional crystalline WSe_2 sheets in the cross-plane direction. On the other hand, it is expected that the in-plane κ is much higher than the cross-plane value because phonons are much less localized in the in-plane direction within each layer of the polycrystalline film.⁶

While the 3ω method⁷ and the time domain thermal reflectance (TDTR) technique⁸ have been widely used to measure the cross-plane κ of thin films, measuring the in-plane κ has been difficult because of parasitic heat conduction in the substrate. Ju *et al.* extended the 3ω method to obtain the in-plane κ of a thin film by using microfabricated heater bridges of varying widths.⁹ The κ of the film was extracted by fitting a two-dimensional heat conduction model to the measurement results. Zink *et al.* obtained the in-plane κ of a thin film evaporated on the back side of a silicon nitride membrane device by comparing the measured thermal conductances before and after the evaporation.¹⁰ Liu and Asheghi patterned a thin Si film into a suspended beam and

employed a metal layer on top of the patterned film as a heater and resistance thermometer.¹¹ The uncertainties of the metal layer thickness and κ introduce uncertainties to the obtained κ of the silicon film.

In this letter, we employ a suspended microdevice to measure the in-plane κ of patterned and suspended WSe_2 and $[(\text{W})_x(\text{WSe}_2)_y]_z$ superlattice films. The measurement results show that the in-plane κ is about 30 times higher than the cross-plane κ obtained by Cahill and co-workers using the TDTR method. The high κ anisotropy is attributed to the in-plane ordered and cross-plane disordered structures of the films. Nevertheless, the in-plane values of the films are still about six times lower than that of compacted single-crystal WSe_2 platelets. Moreover, the additional W layers in the $(\text{W})_x(\text{WSe}_2)_y$ films were found to increase the electrical conductivity to be three orders of magnitude higher than that of the WSe_2 film, but reduce the in-plane lattice thermal conductivity (κ_l) according to an estimation based on the Wiedemann-Franz law.

The WSe_2 films and the $(\text{W})_x(\text{WSe}_2)_y$ superlattice films were synthesized using modulated elemental reactant technique.⁵ The elements were sequentially deposited in a high vacuum chamber (1×10^{-7} Torr background pressure) onto unheated prepolished Si wafer (roughness of ± 3 Å). W (99.95% purity) was deposited at 0.2 Å/s using 3 kW electron beam guns, while Se (99.995% purity) was delivered using a Knudsen effusion cell depositing at 0.5 Å/s. A computer program controlled the thicknesses of the elements deposited, opening a shutter for either a specified period of time or responding to the integrated thickness signal of a quartz crystal monitor. For the superlattice sample measured in this work, approximately four-unit-cell thick W and ten-unit-cell thick WSe_2 were deposited 24 times to produce a

^{a)} Author to whom correspondences should be addressed. Electronic mail: lishi@mail.utexas.edu

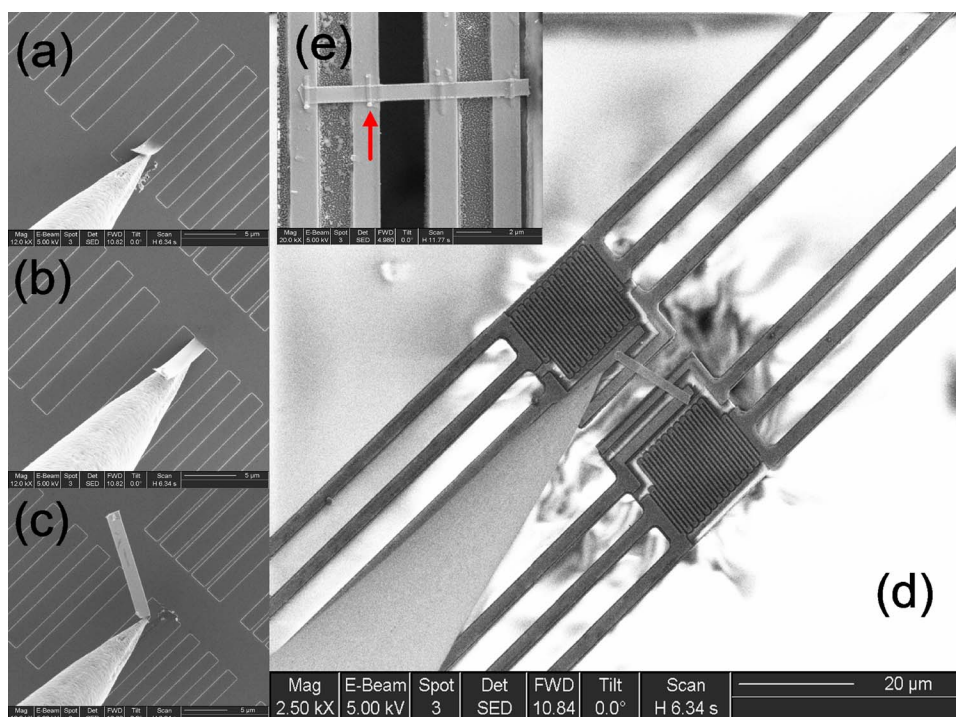


FIG. 1. (Color online) [(a)–(d)] SEMs of the transfer process of a patterned thin film to the microdevice using a nanomanipulator. Prior to film transfer, electron beam lithography was used to pattern arrays of ZEP-520 resist lines on the film, which were used as an etching mask to etch through the film using reactive ion etching with CHF_3 chemistry. The etched film pattern in (a) was obtained after the resist lines were removed using oxygen plasma. (e) SEM of a patterned $(\text{W})_4(\text{WSe}_2)_{10}$ thin film assembled on the microdevice. The arrow indicates one of the four Pt lines deposited on top of the film.

superlattice film. Electron probe microanalysis and Rutherford backscattering measurements show that the repeat thickness of the $\text{W}_4(\text{WSe}_2)_{10}$ layer is 83.6 ± 0.1 Å. After annealing the as deposited amorphous reactants in an open nitrogen atmosphere at 600 °C, the W:Se ratio was found to be 0.93–0.95:2 for the WSe_2 samples.

Individual thin films were patterned using electron beam lithography and reactive ion etching. The patterned thin film was transferred to the suspended microdevice using a sharp tungsten tip actuated by a Zyvx S100 Nanomanipulator System inside a scanning electron microscope (SEM). Because the adhesion between the film and the silicon substrate is very poor, the film could be peeled off by the tip and transferred directly to the suspended microdevice, as illustrated in Figs. 1(a)–1(d). To enhance the electrical and thermal contacts between the film and the microdevice, we used electron beam induced metal deposition to deposit a 250 nm wide, 150 nm thick, 2 μm long Pt line on top of the thin film and each of the four underlying Pt electrodes prepatterned on the suspended device, as illustrated in Fig. 1(e).

After the film was assembled on the microdevice, the etched edge of one suspended $\text{W}_4(\text{WSe}_2)_{10}$ film was analyzed using high resolution transition electron microscopy (HRTEM), which showed, in Fig. 2, moiré fringes indicative of slightly misoriented crystal layers throughout the sample. Tungsten (110) lattice fringes were prominent in the bright field images and it is most likely that these thick W layers are responsible for the linear moiré patterns. Selected area diffraction (SAD) revealed the polycrystalline nature of the superlattice showing a discrete number of comparatively large W grains within the illuminated area. The interplanar spacings of both W and WSe_2 were within 0.5% of those reported for bulk W and WSe_2 by x-ray powder diffraction. Additionally, SAD showed only $\{hk0\}$ reflections from the WSe_2 layer, indicating the $[0001]$ axis perpendicular to the transport direction for the in-plane measurement as expected.

The procedure for measuring the in-plane κ of the film is the same as that for measuring the κ of individual nanowire

using the microdevice consisting of two membrane thermal reservoirs.^{12–15} The data reduction procedure is based on a straightforward one-dimensional heat conduction analysis that does not involve any fitting parameters. In the two-probe thermal measurement procedure based on the suspended device,^{13,14} the obtained κ consists of an error due to the contact thermal resistance between the two membranes and the nanostructure, which is reduced by depositing Pt locally at the two contacts. In a four-probe thermal measurement procedure reported recently,^{12,15} the temperature drops at the two contacts are measured using the nanostructure sample as a thermocouple element so that the error due to contact ther-

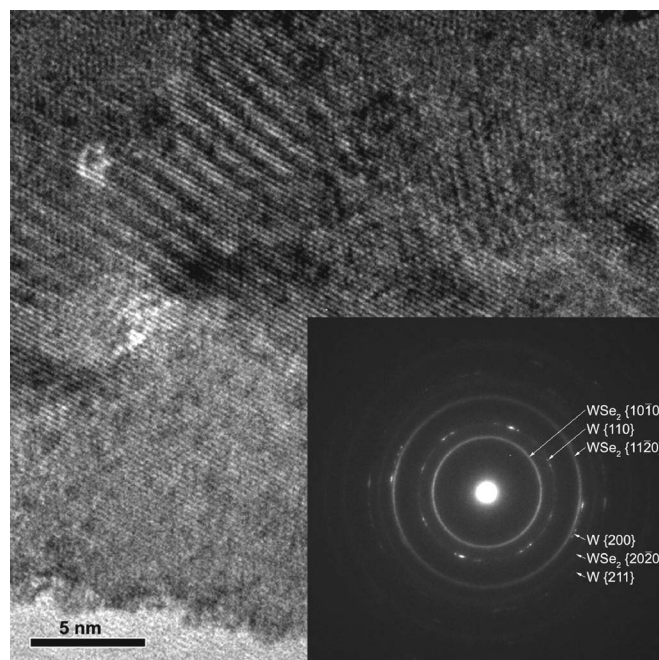


FIG. 2. Top-view HRTEM of the etched edge of a suspended $(\text{W})_4(\text{WSe}_2)_{10}$ film assembled on the microdevice. The inset is the SAD pattern.

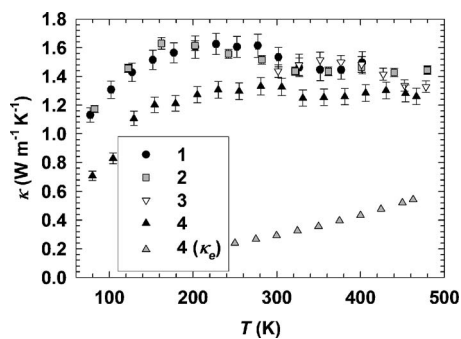


FIG. 3. Measured thermal conductivity of the four thin film samples. Samples 1 and 2 are 162 nm thick WSe_2 film. Samples 3 and 4 are 140 nm thick $(\text{W})_4(\text{WSe}_2)_{10}$ films. Also plotted is the electron contribution (κ_e) to the thermal conductivity of sample 4 estimated from the measured electrical conductivity using the Wiedemann-Franz law.

mal resistance can be eliminated from the obtained κ and Seebeck coefficient of the sample. The four-probe electrical conductivity can also be obtained using the measurement device. However, this four-probe thermal measurement method cannot be applied with great accuracy to the thin film samples measured in this work because the samples have either low Seebeck coefficient or low electrical conductivity and cannot be used to measure the contact temperature drops accurately. The results reported here are thus the two-probe κ . From our previous measurements of other nanofilms¹² and nanofibers,¹⁴ the contact thermal resistance can be about 10%–30% of the total thermal resistance of the sample.

Four thin film samples have been measured. As shown in Fig. 3, the obtained in-plane κ results at room temperature are in the range of 1.2–1.6 $\text{W m}^{-1} \text{K}^{-1}$, which is about 30 times higher than the cross plane κ obtained by Cahill and co-workers using the TDTR method on WSe_2 and $\text{W}_x(\text{WSe}_2)_y$ thin film samples synthesized under the same condition. The anisotropy ratio is much higher than that of compacted single-crystal horizontal WSe_2 platelets, which has an in-plane κ of 9.7 $\text{W m}^{-1} \text{K}^{-1}$ and a cross-plane κ of 2.09 $\text{W m}^{-1} \text{K}^{-1}$. The increased κ anisotropy verifies the in-plane ordered and cross-plane disordered natures of the rotationally disordered layered structure of the films. However, the in-plane κ is still about six times lower than that of the compacted single-crystal platelets. The lower in-plane values in the disordered films could be caused by smaller lateral grain size (about 6–10 nm from both diffraction and TEM measurements), which is evident in the two times lower in-plane electrical conductivity ($0.014 \Omega^{-1} \text{cm}^{-1}$) in the WSe_2 thin film (sample 2) than in the compacted single-crystal WSe_2 platelets. However, the in-plane κ reduction could also be caused by increased scattering of the in-plane phonon modes by the boundaries between adjacent layers in the disordered films.

The measured in-plane κ results of the two WSe_2 samples and one of the two $\text{W}_4(\text{WSe}_2)_{10}$ samples are very similar and slightly higher than that of the other $\text{W}_4(\text{WSe}_2)_{10}$ sample, i.e., sample 4. At room temperature, the in-plane electrical conductivity of sample 4 was found to be about $400 \Omega^{-1} \text{cm}^{-1}$, much higher than the value of $0.014 \Omega^{-1} \text{cm}^{-1}$ for the WSe_2 film (sample 2). Hence, the addition of W layers in the $\text{W}_4(\text{WSe}_2)_{10}$ film increases the electrical conductivity by four orders of magnitude, making the sample metalliclike with a small room-temperature Seebeck coefficient of 1.5 $\mu\text{V}/\text{K}$ relative to the Pt electrode.

For sample 4, the electron contribution (κ_e) to κ can be estimated from the measured electrical conductivity according to the Wiedemann-Franz law. As shown in Fig. 3, κ_e is about one-third of the measured total κ for sample 4 at room temperature. Hence, κ_l contributes to about two-thirds of the total κ of sample 4. Not shown in Fig. 3, the estimated κ_e is about five orders of magnitude lower than the total κ of sample 2 so that κ_l of the WSe_2 sample is essentially the same as the measured total κ . Comparing the deduced κ_l results of the WSe_2 film and the $\text{W}_4(\text{WSe}_2)_{10}$ film, one can note that the addition of W layers in the $\text{W}_4(\text{WSe}_2)_{10}$ film reduces its in-plane κ_l by about 30% compared to the WSe_2 film.

The measurement results show that the in-plane κ of the misoriented layered WSe_2 and $(\text{W})_x(\text{WSe}_2)_y$ superlattice films is about 30 times higher than the cross-plane value. The highly anisotropic κ can be attributed to the in-plane ordered and cross-plane disordered structures of the rotationally disordered films. Nevertheless, the in-plane values of the disordered films are still about six times lower than that of compacted single-crystal platelets. Moreover, it is intriguing to observe that adding W layers in the film could reduce the in-plane κ_l . The lower in-plane values in the film than in the single crystal could be caused by smaller grain size in the films. The further suppression with the addition of W layers in the superlattice films could also be caused by further decrease in the grain size because of strains induced by the additional W layers or by smaller κ_l in the W layers than in the WSe_2 layers. Meanwhile, it is also possible that misorientation of adjacent layers or addition of W layers in the film increases scattering of the in-plane phonon modes by the boundaries between adjacent layers.

This work is supported by ONR (Program manager: Dr. Mihai Gross). M.T.P. is supported by a NSF Graduate Research Fellowship. Nanopatterning was performed at UT Austin Microelectronics Research Center supported by NSF NNIN. We thank David Cahill for suggesting this measurement.

¹T. C. Harman, P. J. Taylor, M. P. Walsh, and B. E. LaForge, *Science* **297**, 2229 (2002).

²R. Venkatasubramanian, E. Siivola, T. Colpitts, and B. O'Quinn, *Nature (London)* **413**, 597 (2001).

³C. Chiriac, D. G. Cahill, N. Nguyen, D. Johnson, A. Bodapati, P. Keblinski, and P. Zschack, *Science* **315**, 351 (2007).

⁴S. Moss, M. Noh, K. H. Jeong, D. H. Kim, and D. C. Johnson, *Chem. Mater.* **8**, 1853 (1996).

⁵M. Noh, C. D. Johnson, M. D. Hornbostel, J. Thiel, and D. C. Johnson, *Chem. Mater.* **8**, 1625 (1996).

⁶K. E. Goodson, *Science* **315**, 342 (2007).

⁷D. G. Cahill, *Rev. Sci. Instrum.* **61**, 802 (1990).

⁸D. G. Cahill, *Rev. Sci. Instrum.* **75**, 5119 (2004).

⁹Y. S. Ju, K. Kurabayashi, and K. E. Goodson, *Thin Solid Films* **339**, 160 (1999).

¹⁰B. L. Zink, B. Revaz, J. J. Cherry, and F. Hellman, *Rev. Sci. Instrum.* **76**, 024901 (2005).

¹¹W. J. Liu and M. Ashghi, *ASME Trans. J. Heat Transfer* **128**, 75 (2006).

¹²A. Mavrokefalos, M. T. Pettes, F. Zhou, and L. Shi, *Rev. Sci. Instrum.* **78**, 034901 (2007).

¹³L. Shi, D. Y. Li, C. H. Yu, W. Y. Jang, D. Kim, Z. Yao, P. Kim, and A. Majumdar, *ASME Trans. J. Heat Transfer* **125**, 881 (2003).

¹⁴C. H. Yu, S. Saha, J. H. Zhou, L. Shi, A. M. Cassell, B. A. Cruden, Q. Ngo, and J. Li, *ASME Trans. J. Heat Transfer* **128**, 234 (2006).

¹⁵F. Zhou, J. Szczech, M. T. Pettes, A. L. Moore, S. Jin, and L. Shi, *Nano Lett.* **7**, 1649 (2007).